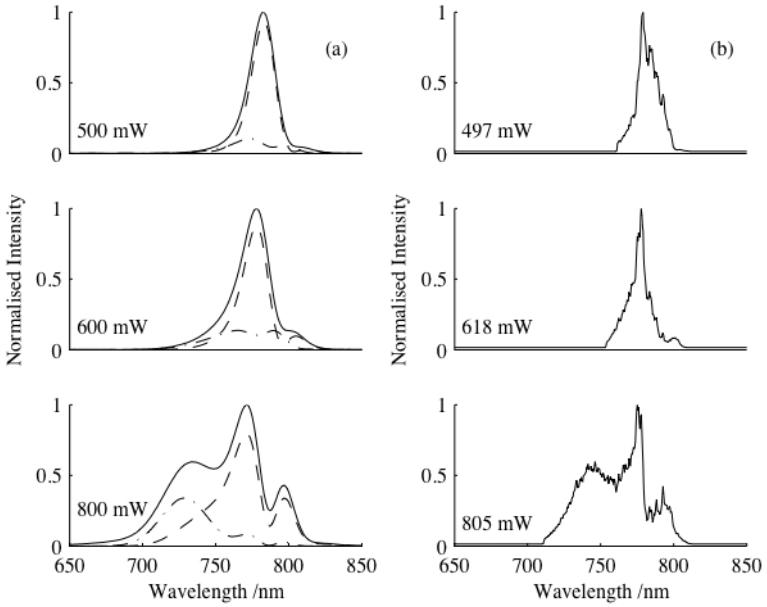

Fig. 2. Predicted (a) and experimental (b) output spectra measured for three input powers, shown. The predicted data shows the total spectrum (solid), as well as those for the EH_{11} (dashed) and EH_{12} (dot dashed) modes. At each laser power, the summed spectral intensity of the modes is normalised to a peak level of 1, as is the experimental data.

Figure 2 shows that at lower powers the EH_{11} mode dominates the spectrum as nonlinear mode coupling is small. The model also predicts a walk-off between the modes, this is calculated to be 8 fs between the EH_{11} and the EH_{12} modes along the 7 cm of the capillary. As the power is increased, more energy is coupled into the EH_{12} and other higher modes. The theoretical model indicates that nonlinear mode coupling is greater at the trailing edge of the pulse due to plasma defocusing, which leads to the observed blue shifted spectra in the higher order modes. Experimentally, the modal distribution cannot be directly determined from a summed spectrum of the kind shown in Fig. 2, although the agreement between theory and experiment allows us to infer that the modal distribution is correct.

In order to test whether the model correctly predicts the distribution of intensity in high order modes, we make use of the fact that as the modes propagate into the far field their spatial divergence is strongly dependent on their order, with higher order modes showing significantly greater angular spread. This means that the radial distribution of the spectral intensities has contributions from different modes at different radii (although the modes are not completely separated). Thus the spatio-spectral intensity distribution in the far field is very sensitive to any variation in the intensities of individual modes, and its measurement can provide a sensitive test of the ability of the numerical model to correctly predict the modal distribution.

Figure 3 shows the calculated (a) and measured (b) spectral intensity distribution as a function of radial distance from the beam axis. The theoretical intensity profiles of the EH_{11} and EH_{12} modes are shown for comparison. It is clear from both theoretical and experimental distributions that the differences in the intensity distributions of the modes are large. The EH_{11} mode has significant contributions at around 790 and 810 nm, and the blue-shifted components at about 740 nm show the same radial profile as the EH_{12} mode, with an on-axis peak, and another ~8 mm from the axis. This distribution is clear in the theoretically modelled intensity distribution. In the measured distributions, the general features of the pattern are

#126971 - $15.00 USD Received 13 Apr 2010; revised 24 May 2010; accepted 27 May 2010; published 4 Jun 2010

repeated. The EH_{11} mode appears at 780 and 810 nm, and the blue-shifted peak at 760 nm has the radially narrower distribution of the EH_{12} mode. However, several differences are clear. The first is that more extensive off-axis blue shifting is seen in the experimental data, implying greater broadening in the higher order modes than was predicted. Secondly, an extra peak can be seen close to the centre of the beam at ~800 nm in the experimental data. The shape of the EH_{11} peaks around 790-810 nm look similar to the spectral distortion caused by SPM, which produces first a splitting, and then a central peak, rising between the split peaks as the nonlinear phase shift increases. Both of these differences suggest that the nonlinear shifting of the spectrum is slightly stronger in the experiment than predicted by theory.

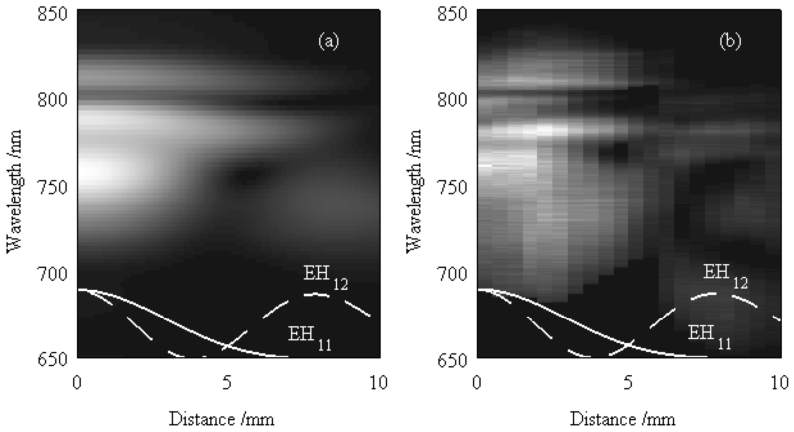

Fig. 3. Predicted (a) and experimental (b) spectral intensity plots in the lambda-r-plane. The solid and dashed white lines show the far-field profiles of the EH_{11} and EH_{12} modes respectively.

While spectral measurements at the capillary exit are a good test of the end point of the model, measurement of the Ar ion fluorescence along the length of the capillary provides a test of the model along the whole propagation length. Experimentally, the fluorescence, produced by excited Ar ions created by the pump pulse, is filtered and imaged from the side. The integrated fluorescence from each point along the capillary length can be compared directly to the ionisation levels predicted by the propagation model.

The integrated argon ion fluorescence and the theoretical integrated ionisation are compared in Fig. 4. The measured 488 nm argon ion fluorescence should be proportional to the calculated ionisation level within the capillary. The beat positions for the EH_{11} and EH_{12} modes calculated for linear propagation are shown as vertical dashed lines; as expected, both experimental and calculated beat positions are clearly shifted from these positions by the effects of nonlinear propagation. The initial increase in ionisation at the capillary entrance is observed in both theory and experiment and the first two major peaks appear at approximately the same positions within the capillary. The smaller structures within these major peaks do not correlate.

#126971 - $15.00 USD Received 13 Apr 2010; revised 24 May 2010; accepted 27 May 2010; published 4 Jun 2010

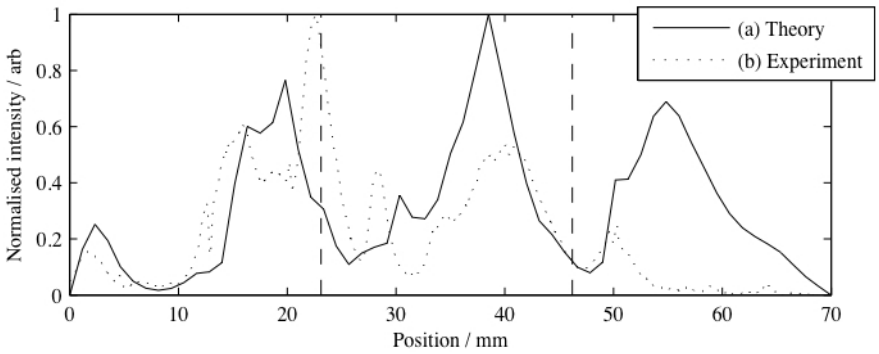

Fig. 4. Comparison of the summed radial ionisation (a) and the imaged argon ion fluorescence (b) along the length of the capillary. The vertical dashed lines show the beat positions for linear mode beating between the EH_{11} and EH_{12} modes.

The final major peak predicted by the numerical model is observed at the same point in the capillary but is significantly smaller in length and size. The discrepancy may be due to losses at the gas inlets within the capillary wall. These have been observed as increased scattering during experiments and are not included within the numerical model.

Conclusion

In this paper we have introduced a new method for numerically modelling nonlinear propagation within a capillary used for HHG. We have compared this model to the spectral output of the capillary and observed strong correlation. The model predicts the modal variation of the pulse shape, and the spatio-spectral measurement technique allows detailed comparison of not just the integrated spectrum, but also the individual modal contributions, because of the differences in the far-field mode patterns, validating the model and the coupling terms chosen. Understanding the modal distribution will allow modelling of XUV phase matching in the presence of nonlinear mode mixing, which is important for XUV generation at high intensities. It will also allow better understanding of the spatial profiles of the compressed pump pulses predicted by the model, providing a route to their exploitation.

Acknowledgments

This research was supported by Research Councils UK Basic Technology Research Programme, Engineering and Physical Sciences Research Council and the University of Southampton.

#126971 - $15.00 USD Received 13 Apr 2010; revised 24 May 2010; accepted 27 May 2010; published 4 Jun 2010